

# Wafer-level vacuum-encapsulated silicon resonators with arc-welded electrodes

George Xereas<sup>1</sup>, Vamsy P. Chodavarapu<sup>2</sup> ✉

<sup>1</sup>Department of Electrical and Computer Engineering, McGill University, Montreal, Quebec H3A0E9, Canada

<sup>2</sup>Department of Electrical and Computer Engineering, Kettering Laboratories, University of Dayton, Dayton, OH 45469, USA

✉ E-mail: vchodavarapu1@udayton.edu

Published in Micro & Nano Letters; Received on 16th May 2017; Revised on 20th July 2017; Accepted on 31st July 2017

This work presents wafer-level vacuum-encapsulated silicon resonators that utilise movable electrodes and arc welding in order to achieve deep sub-micron transduction gaps. The devices are fabricated using micro-electro-mechanical systems (MEMS) integrated design for inertial sensors (MIDIS) process, a commercial pure-play MEMS process, offered by Teledyne DALSA Semiconductor Inc.. The default minimum transduction gap in the MIDIS process is 1.5  $\mu\text{m}$ . Here, the work introduces a technique to permanently reduce the transduction gap of the resonator using localised arc welding to a designed width of  $\sim 200$  nm. The prototype Lamé mode resonators are encapsulated in an ultra-clean 10 mTorr vacuum cavity that ensures long-term stability. The quality factor was measured to be 1.37 million at a resonance frequency of 6.89 MHz. With the narrower gap, the motional resistance of the resonators is reduced by a factor of ten times.

**1. Introduction:** Micro-electro-mechanical systems (MEMS) based oscillators offer several advantages over legacy quartz oscillators including reduced footprint, cost and power consumption [1]. In the era of mobile and wearable devices and Internet-of-Things, further miniaturisation and performance improvements in MEMS resonators for timing applications have been hindered by microfabrication limitations in achieving sub-micron transduction gaps reproducibly and with high yield in a mass-production scale [2].

We have previously described wafer-level vacuum-encapsulated ultra-high quality factor ( $Q$ ) silicon Lamé resonators fabricated using the pure-play MEMS integrated design for inertial sensors (MIDIS) microfabrication process from Teledyne DALSA Semiconductor Inc. (TDSI) [3]. Our previously described prototypes had a transduction gap of 1.5  $\mu\text{m}$  and was characterised with a very high frequency- $Q$  product of  $2.23 \times 10^{13}$  Hz. The large transduction gap necessitated a large 40 V DC polarisation voltage in order to lower the motional resistance. For capacitive transduced resonators, the motional resistance ( $R_m$ ) is proportional to the tesseract of the gap and inversely proportional to the square of the applied polarisation voltage [4]. A narrower gap leads to a much higher output current from the resonator. According to Leeson's linear model of feedback oscillator noise spectrum [5], a higher output current reduces the phase noise of a MEMS oscillator as per the following equation:

$$L(f_{\text{offset}}) = 10 \log \left( \frac{2KTF}{P_{\text{sig}}} \left( \frac{f_o^2}{4Q^2 f_{\text{offset}}^2} + 1 \right) \right) \quad (1)$$

where  $P_{\text{sig}}$  is the signal level coming from the resonant element,  $2KTF$  is the noise of the sustaining electronics,  $Q$  is the quality factor of the MEMS resonator,  $f_o$  is the resonant frequency and  $f_{\text{offset}}$  is the offset frequency at which the phase noise is being measured. Equation (1) shows that an increase in the signal power, or the resonator output current, will result in a drastic decrease of the phase noise for the oscillator.

To this end, researchers have mostly focused on two approaches that included either using advanced microfabrication processes or electrically inducing a smaller gap post-fabrication. Deep-reactive ion etching (DRIE) is widely used for the development of high-aspect ratio MEMS devices, but it is typically limited to an aspect ratio of 20:1 [6], which is the case in the MIDIS process from TDSI. Some research groups have previously

demonstrated aspect ratios on the order of 100:1 with DRIE. However, these modified DRIE processes require either expensive masks with slow etch rates, or a subsequent step of epitaxial silicon growth which make them uneconomical for large-scale mass production [7, 8].

An alternative fabrication method that can produce narrow trenches is high aspect-ratio combined poly- and single-crystal silicon (HARPSS) [9, 10]. However, silicon migration at very high temperatures causes the polysilicon electrodes to roughen which results in electrical shorting issues. Wafer-level bonding typically requires a bonding step under 1100°C, which prohibits the use of HARPSS for trench definition as used in MIDIS process.

Several research groups have pursued gap reduction using movable electrodes [11, 12], where a DC voltage is applied between a stationary and a movable electrode, while a stop island is strategically placed to prevent catastrophic pull-in. This technique has been successfully used to demonstrate sub-micron gaps, but stability issues and the requirement of a high pull-in voltage have limited its commercial viability. In an effort to address this challenge, arc welding has been proposed to permanently fuse the two electrodes together once pull-in was achieved [13, 14]. The latter approach resulted in resonators with high stability and sub-micron trenches. However, the welding depended on the asperity of the surface wall which is difficult to accurately control on a mass-production scale.

Here, we work to limit the influence of surface asperity by designing welding pads that force the welding to occur at a specific small localised area. The multi-project wafer run in MIDIS process provides ten die samples and all ten devices were successfully welded under identical conditions. The current work describes the first demonstration of wafer-level vacuum-encapsulated Lamé square silicon resonator with a deep sub-micrometre transduction gap of  $\sim 200$  nm. The tested devices achieved a  $Q$  of 1.37 million and a ten times reduction in  $R_m$  compared with unmodified devices.

**2. Movable electrodes and arc-welding concept:** A schematic diagram of the Lamé square resonator and the movable electrode configurations is illustrated in Fig. 1. A total of four electrodes are needed for the actuation and sensing of the device, one on each side of the square. The dimensions of the resonator are similar to our previous work [3]. Each electrode is suspended using a spring structure that is 8  $\mu\text{m}$  wide and 570  $\mu\text{m}$  long. Two stop islands are strategically placed within each electrode in order to prevent it

from catastrophically pulling into the resonator during operation as shown in Fig. 2a. From Fig. 2a, each stop island contains two welding pads on its lower side that are  $3\ \mu\text{m}$  wide and  $1.5\ \mu\text{m}$  long. The initial distance between the movable electrode and the resonator is  $1.7\ \mu\text{m}$ , while the distance between the movable electrode and the edge of the welding pad is  $1.5\ \mu\text{m}$ . The distance between the base of the welding pad and the electrode is  $3\ \mu\text{m}$ .

A polarisation voltage of  $50 \pm 0.5\ \text{V}$  between the stop island and the movable electrode results in a pull-in, which reduces the gap between the resonator and the movable electrode to  $\sim 200\ \text{nm}$  (exact value dependent on manufacturing tolerances). Initially, the compliance current of the input power supply is set to  $100\ \mu\text{A}$  and further limited through a  $1\ \text{M}\Omega$  resistor. This allowed repeated pull-in/pull-out cycles without any observable adverse effects. At a later stage, the compliance current is decreased to  $10\ \text{nA}$ , which is high enough to melt the welding pad due to joule heating. The process takes  $\sim 3\ \text{ms}$  and results in a fixed weld. At this point, the transduction gap is permanently reduced to  $\sim 200\ \text{nm}$  and the high DC voltage is not required for operation of the device, and the final configuration is shown in Fig. 2b.

**3. Microfabrication process:** The resonators were fabricated using the standard MIDIS process from TDSI [3, 15]. MIDIS offers a  $30\ \mu\text{m}$  thick single crystal silicon device layer that is wafer-level vacuum encapsulated at  $10\ \text{mTorr}$ . The total leak rate equivalent is noted to be as low as  $6.5 \times 10^{-17}\ \text{atm cm}^3/\text{s}$ , which provides an ultra-clean environment for the long-term operation of the resonators. A scanning electron microscope (SEM) image of the Lamé resonator is shown in Fig. 3. A detailed discussion of the microfabrication process can be found in [15].

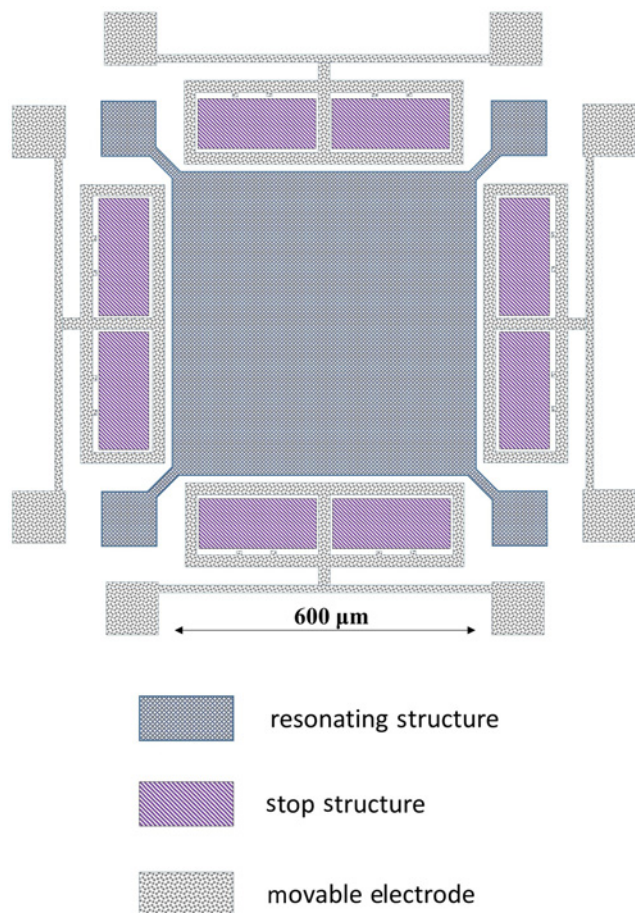


**Fig. 1** Schematic diagram of the Lamé square resonator with the movable electrodes

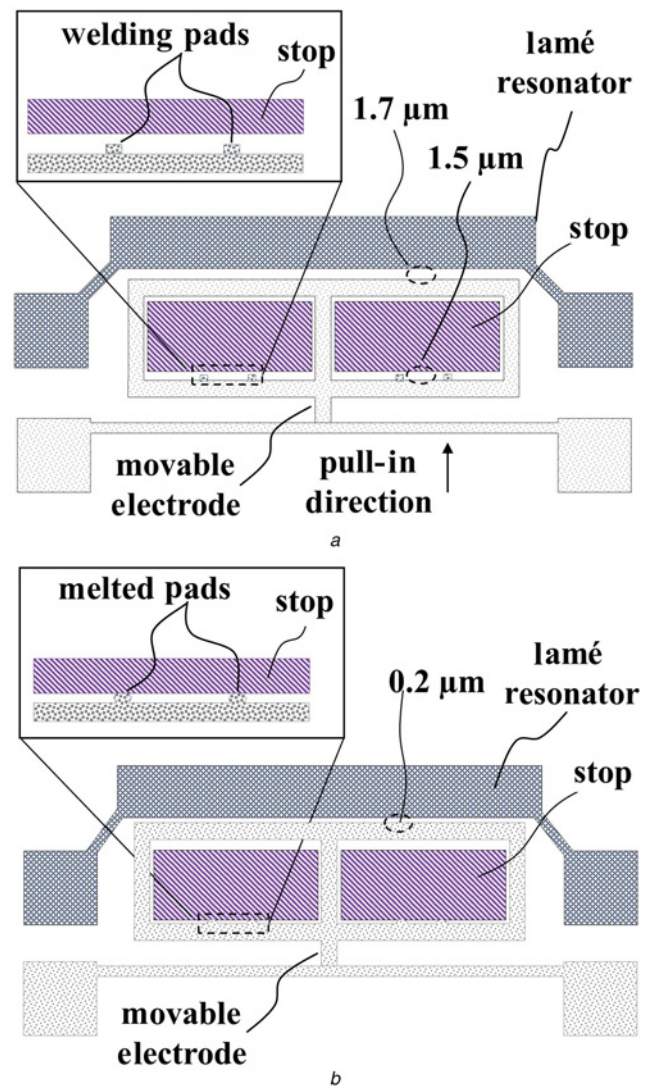


**Fig. 2** Movable electrode configuration  
a Movable electrode configuration pre-welding  
b Movable electrode configuration post-welding

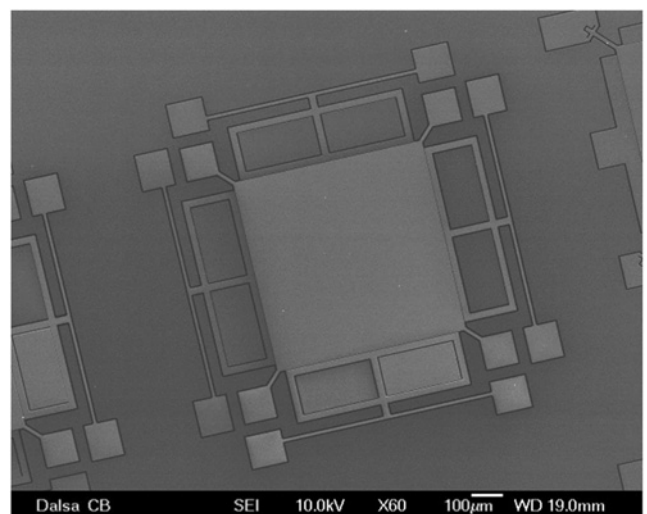


**Fig. 3** SEM of the Lamé-mode resonator that utilises movable electrodes

The high vacuum environment provides a great platform for arc welding as it prevents the growth of native oxide and ensures the surfaces are clean. Arc welding and the concepts described in this work are possible in devices that are exposed to atmospheric pressures. However, it is expected that the welding parameters might vary between devices depending on manufacturing and experimental conditions.

**4. Results and discussion:** A total of ten devices were received from the foundry for this microfabrication run. They were attached to a custom printed circuit board and wire bonded directly to its traces. They were subsequently placed inside a temperature controlled chamber that maintained the temperature constant at  $25^{\circ}\text{C}\pm 0.1^{\circ}\text{C}$ . This is because variations in temperature can affect the parameters of the welding process.

The frequency response of the resonator is measured using a vector network analyser (Keysight Technologies: E5061B). The measurement configuration setup is similar to [3], with the only difference being that the transimpedance amplifiers were replaced by a power combiner. The  $Q$  was measured to be  $1.37 \times 10^6$  and remained largely unchanged after welding. Fig. 4 shows the frequency response of the Lamé resonator before and after the

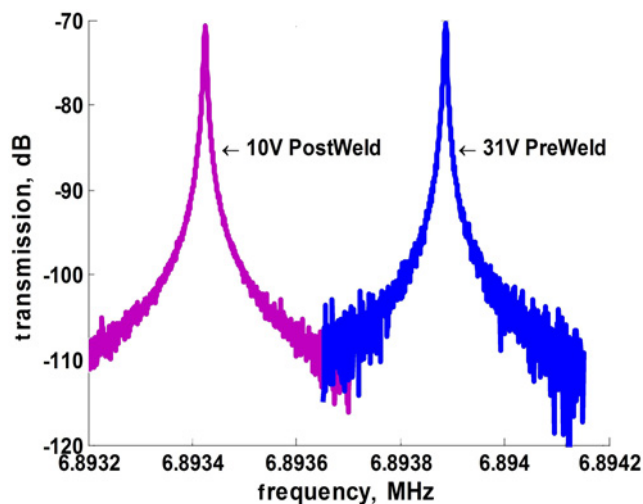


Fig. 4 Frequency response of the Lamé mode before and after the welding has been achieved. The  $Q$  remained largely unchanged at 1.37 million

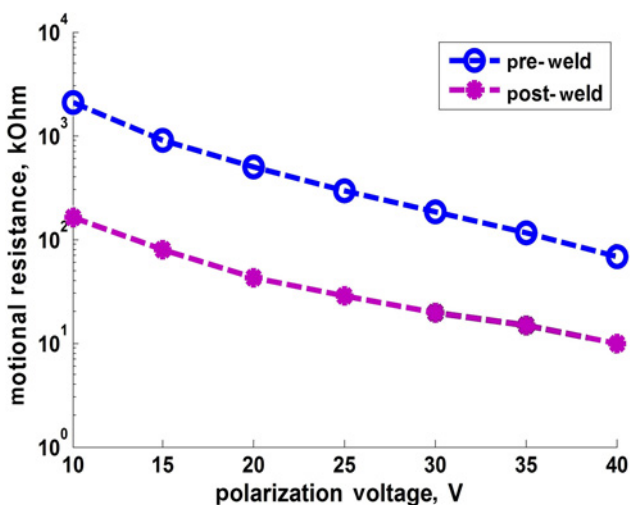


Fig. 5 Comparison of the  $R_m$  of a resonator before and after permanent welding

welding sequence. The resonator with the reduced transduction gap operates at a substantially lower DC voltage. The 70 ppm shift in the resonant frequency can be attributed to a slight change in the electrostatic spring coefficient and temperature variations of the room.

Fig. 5 shows a comparison of the resonator's  $R_m$  before and after welding. A ten times improvement is observed at polarisation voltages ranging from 10 to 40 V. The lowest obtained value was 9.91 k $\Omega$  at 40 V. While, the one order of magnitude reduction in the motional impedance is noteworthy, it is less than what is theoretically possible. Considering that there is a quadratic relation with the transduction gap and the motional resistance, a reduction from 1.7  $\mu\text{m}$  to the designed 200 nm would theoretically lead to a reduction on the order of three orders of magnitude. A probable explanation comes from the fact that the devices are fabricated on an 8' mass-production scale microfabrication process, the manufacturing tolerances including over-etching of the welding pads would affect the final transduction gap and would subsequently lead to a larger gap than the original design. All the ten tested devices showed similar results, which we are assuming to be obtained from the same wafer.

**4. Conclusions:** We presented a wafer-level vacuum-encapsulated Lamé mode silicon resonator fabricated in a commercial pure-play microfabrication with a designed transduction gap on the order of 200 nm. The motional impedance was reduced by an order of magnitude compared with the unmodified device. The described technique can lead to even lower transduction gaps if the mismatch between the resonator-electrode gap and the stop island-electrode gap is further reduced.

**5. Acknowledgments:** This work was generously supported by Natural Sciences and Engineering Research Council of Canada, University of Dayton, and CMC Microsystems.

## 6 References

- [1] Nguyen C.T.C.: 'MEMS technology for timing and frequency control', *IEEE Trans. Ultrason. Ferroelectr. Freq. Control*, 2007, **54**, (2), pp. 251–270
- [2] Fedder G.K., Howe R.T., Liu T.J.K., *ET AL.*: 'Technologies for cofabricating MEMS and electronics', *Proc. IEEE*, 2008, **96**, (2), pp. 306–322
- [3] Xereas G., Chodavarapu V.P.: 'Wafer-level vacuum-encapsulated Lamé mode resonator with f-Q product of  $2.23 \times 10^{13}$  Hz', *IEEE Electron Device Lett.*, 2015, **36**, (10), pp. 1079–1081
- [4] Khine L., Palaniapan M., Lichun S., *ET AL.*: 'Characterization of SOI Lamé-mode square resonators'. Int. Frequency Control Symp., Honolulu, USA, May 2008, pp. 625–628
- [5] Leeson D.B.: 'A simple model of feedback oscillator noise spectrum', *Proc. IEEE*, 1966, **54**, (2), pp. 329–330
- [6] Schilp F.L.A.: 'Method of anisotropically etching silicon'. USA Patent 5501893, March 1996
- [7] Marty F., Rousseau L., Saadany B., *ET AL.*: 'Advanced etching of silicon based on deep reactive ion etching for silicon high aspect ratio microstructures and three-dimensional micro- and nanostructures', *Microelectron. J.*, 2005, **36**, (7), pp. 673–677
- [8] Ng E.J., Chiang C.F., Yang Y., *ET AL.*: 'Ultra-high aspect ratio trenches in single crystal silicon with epitaxial gap tuning'. Proc. of Int. Conf. on Solid-State Sensors, Actuators and Microsystems, Barcelona, Spain, June 2013, pp. 182–185
- [9] Pourkamali S., Hashimura A., Abdolvand R., *ET AL.*: 'High-Q single crystal silicon HARPSS capacitive beam resonators with self-aligned sub-100-nm transduction gaps', *IEEE J. Microelectromech. Syst.*, 2003, **12**, (4), pp. 487–496
- [10] No S. Y., Ayazi F.: 'The HARPSS process for fabrication of nano-precision silicon electromechanical resonators'. Proc. of IEEE Conf. on Nanotechnology, Maui, USA, October 2001, pp. 489–494
- [11] Galayko D., Kaiser A., Buchaillet L., *ET AL.*: 'Design, realization and testing of micro-mechanical resonators in thick-film silicon technology with postprocess electrode-to-resonator gap reduction', *J. Micromech. Microeng.*, 2003, **13**, (1), pp. 134–140

- [12] Shao L.C., Palaniapan M., Khine L., *ET AL.*: 'Micromechanical resonators with submicron capacitive gaps in 2  $\mu\text{m}$  process', *Electron. Lett.*, 2007, **43**, (25), pp. 1427–1428
- [13] Nowack M., Leidich S., Reuter D., *ET AL.*: 'Micro arc welding for electrode gap reduction of high aspect ratio microstructures', *Sens. Actuators A, Phys.*, 2012, **188**, pp. 495–502
- [14] Ng E.J., Yushi Y., Hong V.A., *ET AL.*: 'Stable pull-in electrodes for narrow gap actuation'. Proc. of IEEE Int. Conf. on MEMS, San Francisco, USA, January 2014, pp. 1281–1284
- [15] Xereas G., Chodavarapu V.P.: 'Ultraclean wafer-level vacuum-encapsulated silicon ring resonators for timing and frequency references', *J. Micro/Nanolithography MEMS MOEMS*, 2016, **15**, (3), pp. 035004